3-2005

Simulations of proton order and disorder in ice Ih

Steven W. Rick
University of New Orleans, srick@uno.edu

Recommended Citation

Steven W. Rick. 2005."Simulations of proton order and disorder in ice Ih." Journal of Chemical Physics 122: 094504-1 - 094504-10.

Simulations of proton order and disorder in ice Ih

Steven W. Rick[a)]
Department of Chemistry, University of New Orleans, New Orleans, Louisiana 70148 and
Chemistry Department, Southern University of New Orleans, New Orleans, Louisiana 70126

(Received 9 September 2004; accepted 6 December 2004; published online 25 February 2005)

Computer simulations of ice Ih with different proton orientations are presented. Simulations of proton disordered ice are carried out using a Monte Carlo method which samples over proton degree of freedom, allowing for the calculation of the dielectric constant and for the examination of the degree of proton disorder. Simulations are also presented for two proton ordered structures of ice Ih, the ferroelectric $Cmc2_1$ structure or ice XI and the antiferroelectric $Pna2_1$ structure. These simulations indicate that a transition to a proton ordered phase occurs at low temperatures (below 80 K). The symmetry of the ordered phase is found to be dependent on the water potential. The stability of the two proton ordered structures is due to a balance of short-ranged interactions which tend to stabilize the $Pna2_1$ structure and longer-range interactions which stabilize the $Cmc2_1$ structure. © *2005 American Institute of Physics*. [DOI: 10.1063/1.1853351]

I. INTRODUCTION

In ice Ih, as well as in several other ice phases, there are a number of proton configurations which satisfy the hydrogen bonding requirements.[1,2] The resulting proton disorder gives ice its high dielectric constant and adds extra stability to the solid phase, increasing the melting temperature. It has long been recognized that the proton arrangements are not all energetically equivalent and a small energetic preference for a particular arrangement may give rise to a transition to a proton ordered phase at low temperatures.[3,4] The energetic difference between different proton structures can be described using the geometry of the water dimer (Fig. 1). In the ice Ih lattice, each water molecule forms four hydrogen bonds, one of which is along the c axis. The geometry can be characterized by a torsional angle ϕ along the oxygen–oxygen axis between the C2 axes of the two molecules. For a hydrogen bond along the c axis in ice Ih, the dimer geometry can be either what is termed oblique mirror ($\phi=60°$) or inverse mirror ($\phi=180°$).[3] For the three other hydrogen bonds, along a direction oblique to the c axis, the possibilities are inverse center ($\phi=0°$) and oblique center ($\phi=120°$). The more stable geometries for the dimer are those which place the hydrogens on different molecules away from each other. These are inverse mirror and oblique center.

Protons rearrange in ice with a mechanism involving low concentration orientational defects (the Bjerrum D and L defects) and possibly ionic defects at even lower concentrations.[1,2] The transition to a proton ordered phase is frustrated by the extreme rarity of these defects as the temperature decreases. At low temperatures, the protons may become kinetically trapped in the nonequilibrium proton disordered phase. Proton rearrangement can be enhanced by adding alkali hydroxides. Ordering may also be studied by applying electric fields,[5–8] growing ice on a surface which can promote proton order,[9,10] and examining arctic and antarctic ice.[11–13] In these approaches, there is no agreement about the transition to a low temperature proton ordered phase.[6,10,12–14] Ice crystals doped with alkali hydroxides do exhibit proton mobility and such crystals have been observed to undergo a transition to a proton ordered phase at 71.6 K.[15–20] The transition is first order,[18,21] with an observed volume change,[22] although some authors identify a proton ordering transition as second order.[11,23] The proton ordered phase, termed ice XI, is ferroelectric with a $Cmc2_1$ space group and a net dipole along the c axis. In this structure, all the c-axis hydrogen bonds are inverse mirror and all the others are, interestingly, the presumably higher energy inverse center.[24,25] Thus this proton ordered phase is not what would be predicted based in optimal dimer geometries. A proton ordered structure with a $Pna2_1$ space group in which all hydrogen bonds are inverse mirror and oblique center can be constructed.[26] The $Pna2_1$ structure is antiferroelectric with a zero dipole moment along all lattice directions [see Figs. 2(a) and 2(b)]. The evidence that ice undergoes a transition to a ferroelectric structure in the *absence* of dopants is

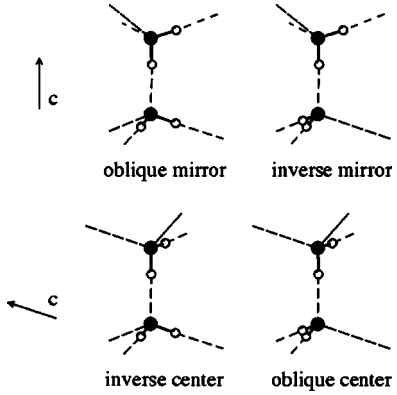

FIG. 1. The possible hydrogen bonds along the c axis (top) and oblique to the c axis (bottom) in the ice Ih lattice. Filled circles represent oxygen atoms and open circles represent hydrogen atoms. Hydrogen bonds to neighboring molecules are shown by the dashed lines.

a)Electronic mail: srick@uno.edu

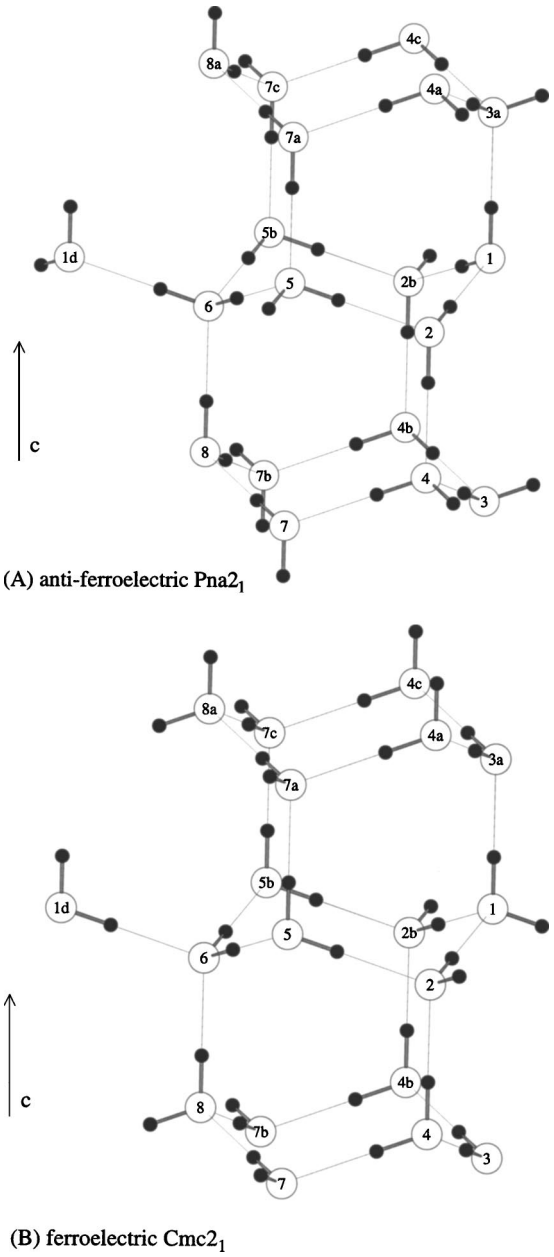

FIG. 2. The ice crystal structure of ice Ih, showing the proton arrangements for the antiferroelectric $Pna2_1$ (a) and ferroelectric $Cmc2_1$ (b) structures. The eight molecules in $Pna2_1$ unit cell are labeled 1–8. The four molecules in the $Cmc2_1$ unit cell are molecules 1–4.

the anisotropy of the dielectric constant.[2,16,21,27,28] The dielectric constant along the c direction, $\epsilon_{\|}$, is greater than along the direction perpendicular to c, $\epsilon_{\perp}$, and the temperature dependence of $\epsilon_{\|}$ goes as $1/(T-\Delta)$. The positive value of the Curie–Weiss temperature, Δ, observed in many studies is indicative of ferroelectric ordering along that direction. The temperature dependence of $\epsilon_{\perp}$ appears to go as $1/T$, indicating no ferroelectric ordering along that direction. On the other hand, one study found no appreciable difference between $\epsilon_{\|}$ and $\epsilon_{\perp}$, with the Curie–Weiss temperature for both being near 0 K.[29]

Computational studies have examined the stabilities of the three structures (disordered, ferroelectric, and antiferroelectric proton ordered ice) using a variety of potential energy models. At the simplest level, interactions are described just as being between point charges on each water molecule.[3,4,23] An initial estimate of the energy difference between the oblique mirror and inverse mirror or inverse center and oblique center is about 1 kcal/mol, just based on the dimer.[3] If nearest neighbors are included the energy differences are much smaller, around 0.2 kcal/mol.[4] For an entire lattice of water molecules interacting only through point charges, the lowest energy proton arrangement is antiferroelectric.[23,30] If quadrupolal interactions are added, then the lowest energy phase can be either ferroelectric or antiferroelectric, depending on the strengths of the quadrupoles.[21,28] *Ab initio* calculations, at the Hartree–Fock level, find that the $Cmc2_1$ and $Pna2_1$ structures are equal in energy.[31] (However, this study found that adding the dopant KOH lowers the energy of the $Cmc2_1$ more than the $Pna2_1$ structure.) Using several water pair potentials, Buch, Sandler, and Sadlej found that the antiferroelectric $Pna2_1$ structure is lower in energy than the ferroelectric $Cmc2_1$ structure but it is not the lowest energy structure found.[32] The lowest energy structure from this study has all c-axis hydrogen bonds as inverse mirror and of the hydrogen bonds oblique to the c axis, one is inverse center and two are oblique centers. Estimates of the stability differences between the proton ordered $Pna2_1$ and proton disordered structures have been made using free energy calculations.[33–39] The more stable structure between proton disordered and the $Pna2_1$ structure is dependent on the potential model used and also, as might not be surprising for systems with both long-range order and electrostatic interactions, on the treatment of long-ranged interactions.[32,34,39] For the SPC/E model,[40] the $Pna2_1$ and proton disordered structures have about the same free energy, with the $Pna2_1$ structure being slightly more stable near the melting point.[34] For the TIP4P model[41] near the melting temperature, studies in which long-ranged interactions have been truncated have found that the $Pna2_1$ proton ordered is more stable than the proton disordered structure,[35,38] while a study using Ewald sums found that the proton disordered structure is more stable.[39] The Sanz *et al.* study reported that the proton ordered $Pna2_1$ phase becomes more stable at very low temperatures (18 K).[39] A similar result is found for the TIP5P model,[42] in which the $Pna2_1$ proton ordered structure is more stable at the melting point when the potential is truncated,[38] but the proton disordered structure is more stable when Ewald sums are used.[39] A further complication is the fact that the disordered structure is commonly treated as a single structure (using, for example, the structures of Hayward and Reimers[43]) while it is by definition an ensemble of different structures.

Computer simulations of ice are limited by a lack of proton mobility due to the absence of the low concentration defects. The arrangement of protons will remain fixed during the duration of the simulation. A recent method has combined strategies for sampling over hydrogen positions[23,44] with conventional Monte Carlo or molecular dynamics methods to allow for the simulation of ice with proton mobility.[45] This method differs from other theoretical approaches to study proton disorder in ice[21,23,28,30,44,46–50] in that since it can be easily combined with molecular dynamics or Monte

Carlo it contains thermal motion of the solid. This study found that for the potentials SPC/E, TIP4P, and TIP4P-FQ (Ref. 51) (with Ewald sums), the protons are disordered except at perhaps low temperatures (around 50 K).[45]

From both the experimental and computational studies, a clear answer to the question of what is lowest energy structure of ice is not apparent. What makes this question particularly difficult is both the lack of proton mobility and the small difference in energies among the different structures. From the experimental data on the transition in doped ice, estimates of the energy difference can be determined. The enthalpy difference ΔH between the disordered and ferroelectric phases of doped ice is dependent on the concentration and type of dopant, suggesting that only a fraction of the proton disordered ice is transformed.[18] The enthalpy changes range from -0.01 to -0.04 kcal/mol (Ref. 18) and if all is transformed, ΔH should be about 0.060 kcal/mol.[52]

This paper aims to add to the understanding of the factors which stabilize the different proton ordered and disordered structures of ice Ih. In this paper, the Monte Carlo method for sampling over hydrogen positions of Ref. 45 is used to examine the structure and energetics of ice Ih using five different water potentials and over a range of temperatures. The structure and energetics of the proton ordered $Pna2_1$ and $Cmc2_1$ structures are examined as well.

II. METHODS

Proton disordered ice is simulated using the algorithm of Rick and Haymet.[45] This method involves two steps, a "walk" step and a "roll" step. In the first step, a hydrogen bonded loop is generated from a random walk on the lattice, which, since the system is finite, is guaranteed to cross itself at some point, creating the loop. In the second step, new hydrogen positions are generated in the loop by rotating or rolling each molecule in the loop around an axis between the oxygen and hydrogen atoms not in the loop. The molecules are rotated by an angle equal to the torsion angle defined by the O–H rotation axis and the oxygen positions of the two neighboring molecules in the loop. This is an angle close to 120°, but will show some variation due to lattice vibrations. The rotations will change the position of the hydrogens in the loop, but will leave the oxygen position and the other hydrogen position the same. Once the new hydrogen positions are generated, the new configuration is accepted based on the usual Metropolis algorithm by comparing the energies of the new and old positions.[53] This method both satisfies detailed balance and is ergodic.[23,45,46] The proton moves are combined with conventional molecular dynamics and a proton move is attempted every 100 time steps. The hydrogen bonded loops can cross over periodic images of the simulation box and, in fact, such loops are critical both for sampling over fluctuations in the dipole moment of the system (needed to calculate the dielectric constant) and for transforming between structures with different net dipole moments (for example, the ferroelectric and antiferroelectric structures). The dielectric constant is calculated from the fluctuations in the total dipole moment of the system as described in Ref. 45. Proton ordered ice was also examined using both the $Cmc2_1$ and $Pna2_1$ structures. In these simulations, no proton moves were attempted and so the hydrogens remain in the original structure for the duration of the simulation.

Systems of ice Ih were simulated using the five different water potentials SPC/E,[40] TIP4P,[41] TIP4P-FQ,[51] TIP5P (Ref. 42) (and the TIP5P-E variant[54]), and NvdE (identified using the initials of the authors).[38] The SPC/E, TIP4P, and TIP5P are among the most commonly used potentials, the TIP4P-FQ potential is polarizable, and NvdE is a new potential developed specifically for ice. The TIP5P-E potential is parametrized to be used with Ewald sums and is a small modification of TIP5P.[54] All simulations used Ewald sums, except as noted below. For comparisons to previous studies, a switching function for long-ranged interactions was used for one study. The simulations were done in the isothermal-isobaric (constant T, P, N) ensemble, by coupling to a pressure bath (at 1 atm) and a Nose–Hoover temperature bath.[55–59] The simulation box is orthorhombic with each side of the box treated as an independent variable for the constant pressure dynamics.[60] A time step of 1 fs was used as well as SHAKE to enforce bond constraints.[61] Simulations were done for systems of 128 and 360 molecules.

III. RESULTS

A. Hydrogen bond order parameters: Temperature dependence, transitions, and energies

The distribution of protons in the ice Ih lattice can be described by hydrogen bond order parameters.[23,45] For the four types of hydrogen bonds shown in Fig. 1, the quantities X_{im}, X_{om}, X_{ic}, and X_{oc} can be defined as the fraction of hydrogen bonds that are inverse mirror, oblique mirror, inverse center, and oblique center. The order parameters will sum to four since there are four hydrogen bonds for each molecule and one has to be either inverse mirror or oblique mirror and the other three must be inverse center or oblique center. Another order parameter can be defined as the fraction of higher energy hydrogen bonds, $(X_{\mathrm{om}}+X_{\mathrm{ic}})/4$. These order parameters allow for easily distinguishing between the various lattice types (see Table I). Table I shows the computed order parameters for the NvdE (Ref. 38) potential over a range of temperatures, the TIP5P (Ref. 42) and TIP5P-E (Ref. 54) potentials at 240 K, and TIP4P (Ref. 41) potential at 25 K. Values for these quantities have been previously reported for SPC/E,[40] TIP4P, and TIP4P-FQ (Ref. 51) in Ref. 45. For all these models, the protons are disordered, except perhaps at low temperatures. At low temperatures, sampling over the proton degrees of freedom becomes inefficient and the protons tend to stay in their original positions.

The TIP4P results at 25 K compliment the earlier results, which went down to a temperature of 50 K.[45] All these simulations find that the ice structure is proton disordered above about 50 K. The simulations presented here as well as in Ref. 45 used Ewald sums. To test the effects of the treatment of long-ranged interactions on the proton positions, an additional simulation was performed for the TIP5P model. In this simulation, the switching function used in Ref. 38 was used rather than Ewald sums. (This simulation used 360 mol-

TABLE I. Hydrogen bond order parameters showing the simulation results at different temperatures and the values for different structures. Numbers in parentheses represent 95% confidence limits.

	T (K)	X_{im}	X_{om}	X_{ic}	X_{oc}	$(X_{om}+X_{ic})/4$
Fully random lattice		0.333	0.667	1.0	2.0	0.417
Antiferroelectric $Pna2_1$		1.0	0.0	0.0	3.0	0
Ferroelectric $Cmc2_1$		1.0	0.0	3.0	0.0	0.75
NvdE	273	0.3601(2)	0.6399(2)	0.9713(3)	2.0288(3)	0.4028(1)
TIP5P	240	0.451(2)	0.549(2)	0.824(1)	2.176(1)	0.3434(7)
TIP5P-E	240	0.447(5)	0.553(5)	0.840(5)	2.160(5)	0.348(2)
NvdE	240	0.3626(3)	0.6374(3)	0.9732(6)	2.0268(6)	0.4027(2)
NvdE	200	0.3628(3)	0.6372(3)	0.9717(3)	2.0283(3)	0.4022(2)
NvdE	150	0.3640(6)	0.6357(7)	0.9700(7)	2.029(1)	0.4014(3)
NvdE	100	0.3674(2)	0.6326(2)	0.9688(8)	2.032(1)	0.4004(2)
NvdE	50	0.3855(5)	0.6145(5)	0.963(1)	2.037(1)	0.3943(3)
TIP4P	25	0.53(1)	0.470(6)	0.806(8)	2.194(8)	0.319(4)
NvdE	25	0.415(4)	0.585(4)	0.955(4)	2.045(4)	0.384(2)

ecules just as in Ref. 38.) The results using the switching function are only slightly different than the results using Ewald and the protons are disordered, with $(X_{om}+X_{ic})/4$ equal to 0.404 ± 0.007. The present results, and the results of Ref. 45, seem clear. When the simulations are started with a proton ordered configuration, they quickly become disordered.

The rapid transition between different structures is illustrated in Fig. 3. Simulations are started in both the ferroelectric $Cmc2_1$ and antiferroelectric $Pna2_1$ structures and are ran at a temperature of 50 K. Within about 500–1000 ps, both simulations have become completely proton disordered, as can be seen by the order parameter $(X_{om}+X_{ic})/4$, as shown in Fig. 3(a). (The progress of the simulation is given by time, even though the evolution of the proton positions is determined by the Monte Carlo moves, not Newtonian dynamics. A Monte Carlo move is attempted every 0.1 ps.) For both simulations, this order parameter is less than the fully random value of 0.417, shown by the dashed line, edging toward the antiferroelectric value of 0 rather than the ferroelectric value of 0.75. For the simulation beginning in the ferroelectric structure, there is a noticeable, and reproducible, lag in the relaxation of the hydrogen bond order parameters. It takes over 100 ps (1000 Monte Carlo attempts) until a move is finally accepted and the proton configuration changes. For the simulation beginning in the $Pna2_1$ structure, moves are accepted after just 12 ps or within 120 attempted moves. Once the first move is accepted from the ferroelectric structure, the other moves are accepted more frequently. The origin of the difference is due to the difference in the type of hydrogen bonded loops that can be constructed for ferroelectric lattice. For that structure, all hydrogen bonds along the c-axis point in the same direction and all hydrogen bonds in a single hexagonal layer are along the same direction as well.[24,25] So a closed hydrogen bonded loop in which each molecule contributes one and only one hydrogen bond to the loop cannot be constructed without crossing to the next periodic image—hydrogen bond paths along any direction are parallel one-way streets in the $Cmc2_1$ structure. In the $Pna2_1$ and proton disordered structure, smaller loops within the central simulation box can be generated and the smaller loops have a higher acceptance probability.[45]

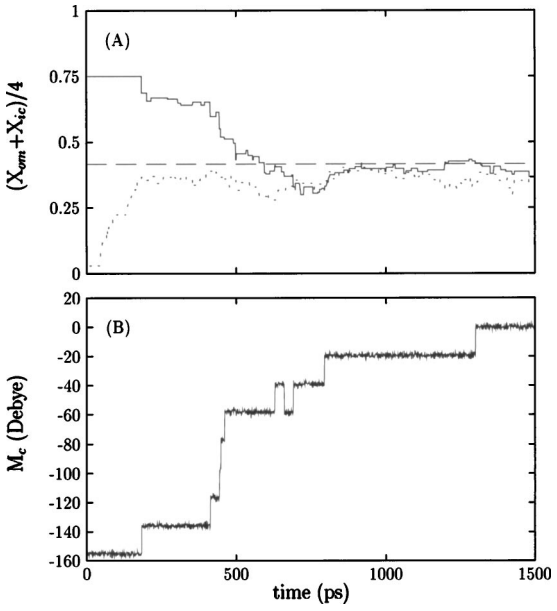

FIG. 3. (a) The evolution of the hydrogen bond order parameter using the TIP4P model, starting with a proton ordered ferroelectric (solid line) and antiferroelectric structure (dashed line), as well as the value for the random lattice (the dotted line at 0.417). (b) The evolution of the total dipole moment of the system starting with a ferroelectric lattice. The temperature is 50 K.

The evolution of the total dipole moment along the c axis, M_c, starting from the ferroelectric lattice is shown in Fig. 3(b). The corresponding plot for the simulation starting from the antiferroelectric lattice is not shown, since it begins at M_c equals zero and simply fluctuates around that value. The simulation starting with the ferroelectric structure begins with a large dipole along the c axis and relaxes to a zero dipole in about 1500 ps. The change in M_c takes place in discrete jumps of about 20 D, which is the amount the dipole moment changes when the hydrogens change position along a path that crosses periodic images. A molecule in a path along the c axis will change from having both hydrogens along the direction oblique to the c axis [like molecule 2 in

TABLE II. Density ρ, lattice constants a and c, and dielectric constant ϵ as a function of temperature for various potential models and from experiment.

	T (K)	ρ (g/cm^3)	a (Å)	c (Å)	c/a	ϵ
NvdE	273	0.915 0(5)	4.519 1(1)	7.378 3(1)	1.633 7(2)	36(1)
Experiment	273	0.917[a]	4.523 2[a]	7.364 6[b]	1.628 2[a]	95[b]
TIP5P	240	0.976 02(1)	4.421 8(5)	7.224 1(1)	1.633 7(2)	30(3)
TIP5P-E	240	0.976 64(1)	4.420(1)	7.223(2)	1.634(1)	30(2)
NvdE	240	0.923 0(5)	4.506 38(2)	7.357 88(3)	1.632 77(1)	42(1)
Experiment	240	0.922	4.515 9	7.352 2	1.628	109
NvdE	200	0.932 0(5)	4.492 25(3)	7.335 14(1)	1.632 84(1)	52(2)
Experiment	200	0.926	4.508 0	7.339 8	1.628 2	130
NvdE	150	0.941 7(3)	4.475(2)	7.307(3)	1.633(1)	67(1)
Experiment	150	0.931	4.500 8	7.327 7	1.628 1	174
NvdE	100	0.951(1)	4.462(1)	7.285(1)	1.633(1)	101(4)
Experiment	100	0.934	4.496 6	7.319 8	1.627 7	
NvdE	50	0.960(1)	4.448(1)	7.263(1)	1.633(1)	184(14)
Experiment	50	0.934	4.496 5	7.320 5	1.628 0	
NvdE	25	0.964(1)	4.440(1)	7.253(1)	1.634(1)	299(31)
TIP4P	25	0.970 0(3)	4.223 0(6)	7.259 3(7)	1.719 0(3)	216(55)
Experiment	25	0.933	4.496 7	7.320 5	1.628	

[a]Reference 63.
[b]Reference 17.

Fig. 2(b)] to having one hydrogen pointing straight down along c axis [like molecule 2 in Fig. 2(a)]. The change in the dipole moment for such a move can easily be found, assuming a perfectly tetrahedral lattice. The dipole moment along the c axis, μ_c, is dependent on the angle between the dipole moment vector and the c axis. For the initial position, this angle is equal to 109.47/2, pointing upward, and so the c component of dipole moment of that molecule is equal to $\mu\cos(109.47/2)$, where μ is the magnitude of the dipole moment of the molecule. After the hydrogen switches position, the dipole moment vector now makes an angle 109.47/2 with the c axis in the downward direction and so μ_c equals $-\mu\cos(109.47/2)$. The change is then $2\mu\cos(109.47/2)$. Other molecules in the same path will make an opposite kind of switch from one hydrogen pointed upward along the c axis to both pointing obliquely (like molecule 4). This switch will have the same change in the dipole moment. For the 128 molecule unit cell, it takes 8 molecules to cross to the next periodic cell in the c axis, so the change in M_c will be $16\mu\cos(109.47/2)$, which is equal to 20 D for the TIP4P model in which μ is equal to 2.177 D.[41] (The path could takes turns oblique to the c axis, but this will not affect M_c.)

From Table I, it can be seen that the proton configurations are not completely random and that there is a preference for inverse mirror and oblique center hydrogen bonds, consistent with other studies.[3,4,23,45] This preference gets stronger at lower temperatures and from the temperature dependence of the order parameters, estimates of the energy difference between the different types of hydrogen bonds can be made.[45] The ratio of the order parameters can be written as

$$\frac{X_{\mathrm{im}}}{X_{\mathrm{om}}} = \frac{1}{2}e^{-(\langle E_{\mathrm{im}}\rangle - \langle E_{\mathrm{om}}\rangle)/kT} \tag{1}$$

and

$$\frac{X_{\mathrm{ic}}}{X_{\mathrm{oc}}} = \frac{1}{2}e^{-(\langle E_{\mathrm{ic}}\rangle - \langle E_{\mathrm{oc}}\rangle)/kT}, \tag{2}$$

where the prefactor of 1/2 is due to there being twice as many oblique as inverse hydrogen bonds and $\langle E_\alpha\rangle$ is the average energy of type α hydrogen bonds. Values of $\langle E_{\mathrm{om}}\rangle - \langle E_{\mathrm{im}}\rangle$ and $\langle E_{\mathrm{ic}}\rangle - \langle E_{\mathrm{oc}}\rangle$ have been determined using this method for the TIP4P and TIP4P-FQ models.[45] For the NvdE model, $\langle E_{\mathrm{om}}\rangle - \langle E_{\mathrm{im}}\rangle$ is 0.01 kcal/mol and $\langle E_{\mathrm{ic}}\rangle - \langle E_{\mathrm{oc}}\rangle$ is 0.002 kcal/mol. The values from Ref. 45 for $\langle E_{\mathrm{om}}\rangle - \langle E_{\mathrm{im}}\rangle$ are 0.03 (TIP4P) and 0.08 kcal/mol (TIP4P-FQ) and for $\langle E_{\mathrm{ic}}\rangle - \langle E_{\mathrm{oc}}\rangle$ are 0.008 (TIP4P) and 0.04 kcal/mol (TIP4P-FQ), all of which indicate how small the energy differences are between the different hydrogen bond types.[62] All models find that the inverse mirror and oblique center hydrogen bonds are lower in energy.

B. Properties of the ice Ih lattice: Energy, dielectric constant, and lattice constants

Other properties as given by the different potential models are listed on Table II. The data are compared to the experimental data, which for some temperatures are interpolations between interpolated data points. The experimental value for the dielectric constant is found using the formula from Johari and Whalley, $\epsilon = \epsilon_\infty + 24620/(T-6.2)$, where ϵ_∞ is the infinite frequency dielectric constant taken to be 3.2.[17] For the density and lattice constants, the NvdE model gives good values at higher temperatures. The NvdE model is one of the few potentials that was parametrized for ice and so the agreement is by design.[38] At lower temperatures the agreement is not as good and a negative thermal expansivity is not reproduced. Other models developed for liquid water, including the TIP5P (and TIP5P-E) data reported here, give densities which are too high. This has been shown for SPC/E model,[37,64,65] TIP4P,[35,65] TIP4P-FQ,[66] as well as other

TABLE III. Properties at a temperature of 25 K for ice Ih as predicted from different potential models and as given by experiment for different proton configurations.

Property	Proton symmetry	SPC/E	TIP4P	TIP4P-FC	TIP5P-E	NvdE	Experiment
ρ g/cm^3	Disordered	0.9752(4)	0.9701(4)	1.0215(2)	1.0370(2)	0.9656(1)	0.933[a]
	$Pna2_1$	0.9792(4)	0.9720(4)	1.0254(9)	1.0387(2)	0.9661(2)	
	$Cmc2_1$	0.982(1)	0.9710(8)	1.0211(8)	1.0451(2)	0.9670(1)	0.934[b]
a (Å)	Disordered	4.427(1)	4.420(1)	4.3461(4)	4.3789(3)	4.441(1)	4.4967[a]
	$Pna2_1$	4.633(1)	4.417(1)	4.37(1)	4.4520(2)	4.3955(3)	
	$Cmc2_1$	4.2162(2)	4.3548(3)	4.303(2)	4.068(1)	4.514(1)	4.467[b]
c (Å)	Disordered	7.223(1)	7.270(1)	7.1249(5)	7.0807(6)	7.248(1)	7.3205[a]
	$Pna2_1$	7.183(1)	7.264(3)	7.104(6)	7.0749(7)	7.2503(3)	
	$Cmc2_1$	7.128(5)	7.3110(6)	7.144(8)	7.0745(2)	7.2459(6)	7.292[b]
c/a	Disordered	1.6316(4)	1.6448(4)	1.6394(2)	1.6170(2)	1.6321(4)	1.6280[a]
	$Pna2_1$	1.5504(4)	1.6446(8)	1.625(5)	1.5892(2)	1.6495(1)	
	$Cmc2_1$	1.691(1)	1.679(1)	1.660(2)	1.7391(7)	1.6054(4)	1.632
E (kcal/mol)	Disordered	−14.541(1)	−13.479(1)	−14.024(1)	−14.123(1)	−14.069(1)	−14.09[c]
	$Pna2_1$	−14.576(1)	−13.485(1)	−14.00(1)	−14.187(1)	−14.075(1)	
	$Cmc2_1$	−14.563(4)	−13.479(1)	−13.969(6)	−14.164(1)	−14.083(1)	−14.15[d]
X_{im}	Disordered	0.532(4)	0.442(5)	0.669(2)	0.736(5)	0.46(2)	
X_{om}	Disordered	0.468(4)	0.558(5)	0.331(2)	0.264(6)	0.54(2)	
X_{ic}	Disordered	0.73(1)	0.751(5)	0.770(1)	0.618(3)	0.90(2)	
X_{oc}	Disordered	2.27(1)	2.249(5)	2.230(2)	2.382(3)	2.10(2)	
$(X_{\mathrm{om}}+X_{\mathrm{ic}})/4$	Disordered	0.300(4)	0.327(1)	0.275(1)	0.220(2)	0.360(7)	

[a]Reference 63.
[b]Reference 22.
[c]Reference 72.
[d]Reference 52.

models.[65] The differences between the TIP5P and TIP5P-E models are small, unlike in the liquid phase for which density is different by over 10%.[54,67]

The calculated dielectric constant for the NvdE and TIP5P models are much lower than the experimental values. This is consistent with the results for the other nonpolarizable potentials TIP4P and SPC/E.[45] The NvdE model results for ice are also consistent with the model's predicted value for the liquid, 33 ± 7.[38] The small dielectric constant may be due to an underestimation of the water molecule's dipole moment.[44,68–71] The polarizable TIP4P-FQ model, which has a larger dipole moment, has a dielectric constant close to the experimental value for ice,[45] as well as the liquid.[51] The low value of ϵ for TIP5P and the TIP5P-E models is not consistent with the predicted values for the liquid, around 80.[42,54] For liquid, the TIP5P and TIP5P-E models give a larger ϵ than other models with similar dipole moments because they have a relatively small quadrupole.[54] In ice, the TIP5P model has a smaller ϵ than other models with similar dipole moments. The difference in the predicted dielectric constant for ice and liquid water illustrates that the dielectric response follows different mechanisms in the two phases.

All the results presented above are for the 128 molecule system, with the exception of the one TIP5P simulation with the switching function. The smaller system size makes the calculation of the dielectric constant much quicker.[45] The data presented below are generated using a 360 molecule system.

C. Low temperature properties of the different ice structures

To examine the low temperature properties of the various water models with different proton structures, simulations were run at a temperature of 25 K (Table III). As mentioned previously for the higher temperatures, all models give densities which are too large. The models do not give a clear trend for the changes in the lattice constants. The TIP5P-E model gives a very large difference in a between $Cmc2_1$ and the other two structures. The values for the ratio c/a also vary considerably, with values both well above and below the value for an ideal tetrahedral lattice, 1.632 99.

The hydrogen bond order parameters for the various models at 25 K are given in Table III. All the values demonstrate a shift away from a completely random lattice with a greater preference for inverse mirror and oblique center hydrogen bonds. The TIP5P-E model has values which are the farthest from the random models studied. The NvdE model is the closest to random. A greater deviation from the random values indicates a bigger energy difference between the various types of hydrogen bond geometries [as indicated by Eqs. (1) and (2)]. The values for the order parameters are consistent with those from previous studies which used Monte Carlo methods to sample proton configurations.[23,45] These values are different from the structure identified by Buch, Sandler, and Sadlej as a minimum energy structure for several water potentials. That structure has $X_{\mathrm{im}}=1$, $X_{\mathrm{om}}=0$, $X_{\mathrm{ic}}=1$, $X_{\mathrm{oc}}=2$, and $(X_{\mathrm{om}}+X_{\mathrm{ic}})/4=1/4$.

The energies of the different structures are given in Table III as well. The experimental value quoted for the disordered structure is the lattice energy estimate from Whalley,[72] and the value for the $Cmc2_1$ structure is that value minus the enthalpy change between the two structures (0.060 kcal/mol).[18,32,52] For the TIP4P-FQ model, the proton disordered structure is lowest in energy, slightly lower in energy than the $Pna2_1$ structure. For this model and three others, the

$Pna2_1$ structure is lower in energy than the $Cmc2_1$ structure, consistent with previous simulations.[32] In contrast, the NvdE model predicts that $Cmc2_1$ is the lowest energy structure. This is surprising because no previous study with empirical water potentials found the ferroelectric $Cmc2_1$ structure to be more stable. In addition, the results are an apparent contradiction to the results presented above. A significant difference between the $Cmc2_1$ and $Pna2_1$ structures is the fraction of hydrogen bonds that are inverse center (see Table I). The results presented for the NvdE model find that in the disordered lattice, the energy of the inverse center is above the energy of the oblique center hydrogen bond, making it puzzling why a structure with all inverse center hydrogen bonds ($Cmc2_1$) should be lower in energy than a structure with all oblique center hydrogen bonds ($Pna2_1$).

D. Stabilization of the $Cmc2_1$ relative to the $Pna2_1$ structure

To illustrate how the different models can predict different structures to be the most stable, despite the fact that all models predict that inverse center hydrogen bonds are higher in energy, it is helpful to consider the interaction energies as a function of the distance on the lattice. For a perfectly tetrahedral lattice, coordination shells around a water molecule can be constructed.[44] For example, there are 4 nearest neighbors (the first coordination shell) and 12 next nearest neighbors (the second coordination shell). Using Ewald sums, the Coulombic interaction is split into a real space part and a Fourier space part. The Fourier space part is small for both structures (less than 0.31 cal/mol). The average energy between a molecule and those molecules in its nth coordination shell is shown in Fig. 4(a) for the NvdE model and Fig. 4(b) for the TIP5P-E model. This energy is the sum of the Lennard-Jones and the real space Ewald interactions, as given by

$$E_{ij} = \sum_{a,b} 4\epsilon_{ab}\left[\left(\frac{\sigma_{ab}}{r_{ia,jb}}\right)^{12} - \left(\frac{\sigma_{ab}}{r_{ia,jb}}\right)^{6}\right] + q_a q_b \mathrm{erfc}(\lambda r_{ia,jb})/r_{ia,jb}, \quad (3)$$

where the sum is over the atoms a and b on molecules i and j, $r_{ia,jb}$ is the distance between the atoms, σ_{ab} and ϵ_{ab} are the Lennard-Jones parameters, q_a and q_b are the charges, erfc is the complimentary error function, and λ is the screening parameter set equal to $5/L$, where L is the simulation box side length. The contributions to the energy will depend on the value of λ used, but the total energy will not. For the first two coordination shells, the contributions from molecules in different hexagonal layers, involving displacement along the c axis (denoted c), and those in the same hexagonal layer (denoted h, are shown separately. For both lattices, the hydrogen bond along the c axis (for example, between molecules 2 and 4 in Fig. 2) is inverse mirror and has about the same energy. The hydrogen bonds oblique to the c axis (between molecules 1 and 2, for example) are inverse center for the $Cmc2_1$ lattice and oblique center for the $Pna2_1$ lattice. For both models, the oblique center is lower in energy, although the difference is greater for the TIP5P-E model. For the second nearest neighbors, the contribution for individual

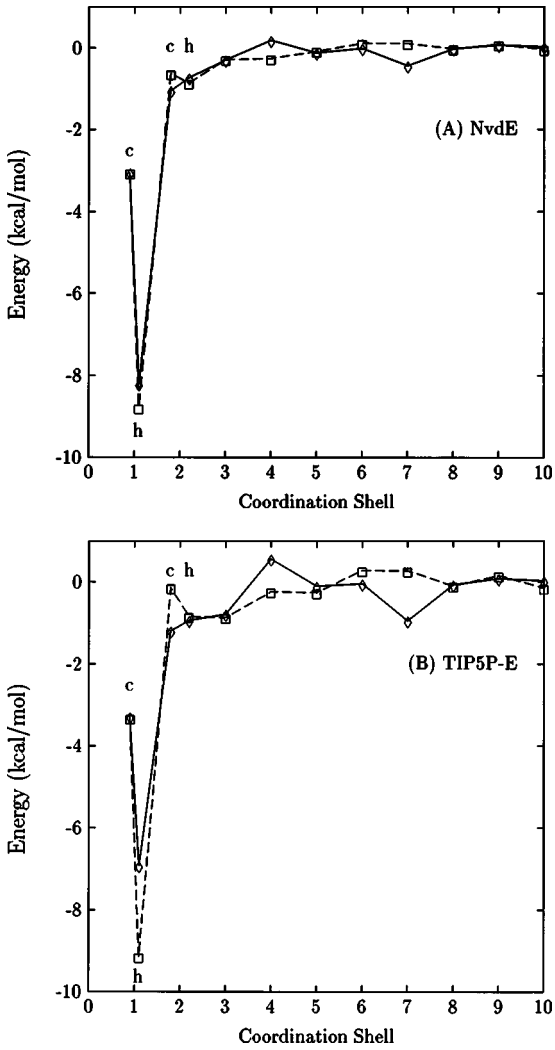

FIG. 4. The interaction energy as a function of coordination shell for the (a) NvdE model (Ref. 38) and the TIP5P-E model (Refs. 42 and 54) models. This is the sum of the Lennard-Jones plus the real space part of the Ewald interactions for water molecules in the ice Ih lattice. For the first two coordination shells, the interactions are separated into neighbors in the same hexagonal layer (h) and those up or down along the c axis (c). Energies are shown for the antiferroelectric $Pna2_1$ (squares and solid line) and ferroelectric $Cmc2_1$ lattices.

neighbors in the same hexagonal layer (labeled 2h, for example, molecules 1 and 5 or 2 and 6 in Fig. 2) are different for the two structures, but they average to about the same value. There are six molecules among the second nearest neighbors involving molecules in different hexagonal layers (labeled 2c in Fig. 4). Of the six, two of the interactions are higher in energy for the $Cmc2_1$ structure (like those between molecules 4 and 5 or 2 and 7), some are lower (molecules 1 and 4 or 2 and 3), and some are about the same (1 and 4a, 1 and 4b, or 3 and 2b). On average, the interactions are slightly lower for the $Cmc2_1$ structure. This difference in energy only partially compensates for the higher energy of the nearest neighbors for the $Cmc2_1$ structure. Just from a consideration of nearest and second nearest neighbors both the NvdE and TIP5P-E models predict that the $Cmc2_1$ structure is higher in energy.

The next coordination shell only contains one molecule, directly above or below along the c axis (molecules 5 and 7

or 2 and 4a). The geometry of this pair is the same for both structures and the energies are the same. A significant difference appears for the fourth coordination shell, which contains nine molecules, three in the same hexagonal layer (molecules 1 and 6 or 2 and 5b) and six in different layers (4 and 6 or 2 and 8). Of the interactions in the same hexagonal layer, one-third of them are slightly more stable (for example, between molecule 1 and 6) for the $Cmc2_1$ structure (this is an attractive interaction), while two of them (as between 2 and 5b or 5 and 2b) are slightly more stable for the $Pna2_1$ structure (this is a repulsive interaction). For the six interactions in different hexagonal layers, two are about equal in energy for the different structures (repulsive interactions between molecules 2 and 4b or 4 and 2b) and four are lower in energy for the $Pna2_1$ structure (between 1 and 7a or 5 and 3b, which are slightly attractive in the $Pna2_1$ and slightly repulsive in the $Cmc2_1$ structure).

The interactions that appear to play a key role in stabilizing the $Cmc2_1$ structure are between molecules in the seventh coordination shell. There are nine molecules in this shell, six in the same hexagonal layer (molecules 2 and 1d) and three in different (molecules 4 and 7a or 4 and 3a). Of the six in the same hexagonal layer, two are more stable for $Pna2_1$ structure (for example, between molecule 1 and a molecule shifted one unit cell forward or backward along the a or [100] direction from the position of molecule 2). The other seven interactions are all lower in energy for the $Cmc2_1$ structure. That these interactions are lower in energy for the $Cmc2_1$ structure is apparent from considering the interactions between molecules 2 and 1d, molecules 4 and 3a, and molecules 8 and 7a in Figs. 2(a) and 2(b). In Fig. 2(a), the molecules are arranged with a single hydrogen atom between the oxygen atoms, while in Fig. 2(b), there are either no hydrogens (pairs 2 and 1d, 4 and 3a) or two hydrogens (8 and 7a) between the two molecules. The interactions of this coordination shell are what brings the energies of the two structures close together. In the case of the NvdE model, the difference in the dimer energy between the inverse center hydrogen bonds (present in the $Cmc2_1$ structure) and oblique center hydrogen bonds (present in the $Pna2_1$ structure) is small enough so that the gain in energy due to seventh coordination shell is enough to make the $Cmc2_1$ structure lower in energy. For TIP5P-E, and the other models, the energy difference between inverse and oblique center is too great to be compensated for by the longer-range interactions. Coordination shells larger than seven do not contribute as significantly to the energy due to the greater separations between molecules and the damping of the interactions by the complementary error function [see Eq. (3)].

The balance between short- and long-range interactions explains the puzzle mentioned above, that for the proton disordered lattice switching one hydrogen bond from oblique center to inverse center increases the energy, but if all hydrogen bonds are inverse center, then the energy is decreased. It is only stable if the lattice is structured so that the favorable interactions with the seventh coordination shell are present. The study of Buch, Sandler, and Sadlej for cubic ice also showed that while the nearest neighbor interactions favor the $Pna2_1$, the longer-range interactions decrease the relative stability between the $Pna2_1$ and $Cmc2_1$ structures.[32] Particular stability is added to the $Cmc2_1$ structure from the combination of the third and fourth nearest neighbors. These coordination shells of the cubic lattice occur at the same distance as the fourth and fifth shells of the hexagonal lattice.[44] Unlike the cubic structure, for the hexagonal lattice these shells do not stabilize the $Cmc2_1$ structure and, in fact, the fourth shell stabilizes the $Pna2_1$ structure (Fig. 4). Therefore, the stabilization of the $Cmc2_1$ structure comes from different coordination shells in the cubic and hexagonal lattices.

IV. CONCLUSIONS

The results of the preceding section, as well as those of Ref. 45, indicate those of the five potential models studied (SPC/E, TIP4P, TIP5P, TIP4P-FQ, and NvdE) are proton disordered down to a very low temperature. This is consistent with the experimental structure of ice Ih and with free energy calculations which find the proton disordered structure is stable down to 18 K.[39] Other free energy calculations, for SPC/E,[37] TIP4P,[35,38] and TIP5P,[38] have found that the proton ordered phase is more stable than the disordered phase. This may be due to the use of cutoffs rather than Ewald,[34,39] although our simulation using cutoffs predicts that the proton disordered structure is more stable. The free energy calculations are for one particular proton disordered configuration, which may not be the most stable disordered form. In addition, small differences in stabilities may be hard to resolve with the free energy calculations. At all but the lowest temperatures, a proton disordered structure will spontaneously form from an initial ordered phase (see Fig. 3).

The calculated dielectric constants agree with previously calculated values[45] and indicate that for the nonpolarizable models SPC/E, TIP4P, TIP5P, and NvdE the dielectric constants are all considerably underestimated, by about a factor of 3. The polarizable TIP4P-FQ model accurately predicts the dielectric constant of ice.[45] Some of the nonpolarizable models do give fairly accurate dielectric constants for the liquid, most notably the TIP5P model. Properties of the water models which influence the dielectric constant (for example, the dipole[73–75] and the quadrupole moments[54,76]) apparently do so in different ways for the liquid and solid. The sharp difference between the predicted values with the same model for the two phases [for example, the TIP5P model gives a dielectric constant near 80 for the liquid at 298 K (Ref. 42) and about 30 for ice at 240 K] is due to the different mechanism of the dielectric response for the liquid and the solid.

At a temperature of 25 K, an ordered phase has a lower energy than the proton disordered phase for four of the potential models (Table III). One of the models, the NvdE model, predicts that the $Cmc2_1$ is the minimum energy structure, while the other three predict that minimum energy structure is $Pna2_1$. No other model has been shown to give the $Cmc2_1$ as the lowest energy structure. For the TIP4P-FQ model, the proton disordered is slightly more stable than either of the ordered phases. All of the energy differences between the different structures are small, comparable to the experimental estimate of the energy difference between the disordered and $Cmc2_1$ structure of 0.06 kcal/mol.[18,32,52]

From the value of the energy difference between the ordered and disordered structures, ΔE, an estimate of a transition temperature T_M from proton disordered to proton ordered ice can be estimated from[4]

$$T_M = \Delta E/\Delta S, \tag{4}$$

where ΔS is the entropy change between the two structures, assumed to be the residual entropy (0.81 cal/mol/K), and the small contribution to the enthalpy from differences in the density are neglected. The values for T_M vary over a 70 K temperature range (TIP4P, 7 ± 2 K; NvdE, 20 ± 2 K; SPC/E, 43 ± 5 K; TIP5P-E, 79 ± 2 K). The experimental value, for doped ice, is 71.6 K.[15–20] This is a transition to the $Cmc2_1$ structure, which is the structure predicted by the NvdE model.

The relative stability of the different structures is due to a balance of short- and long-range interactions. Nearest neighbor interactions favor the $Pna2_1$ structure,[26] which has all hydrogen bonds oblique to the c axis as oblique center, while the $Cmc2_1$ structure has all hydrogen bonds oblique to the c axis as inverse center (see Fig. 1). The inverse center hydrogen bonds are higher in energy.[3,4] The $Cmc2_1$ structure is stabilized by interactions with second nearest neighbors (the second coordination shell) and, most importantly, with molecules in the seventh coordination shell (see Fig. 4). The distance between molecules in the seventh coordination shell is $r_7=(57/9)^{1/2}\,r_1$, where r_1 is the distance between nearest neighbors.[44] Using $r_1=2.75$ Å, we obtain that r_7 is 6.9 Å. The competition between the short-range and the long-range interactions means that the stability of the different structures is very sensitive to details of the potential models, as well as the treatment of long-range electrostatics. It is possible, as well, that the balance of these interactions may be shifted by methods used to examine proton structure at low temperatures, including doping by alkali hydroxide,[15–20] growing ice crystals next to solid surfaces,[9,10] and applying electric fields.[5,6] The determination of the minimum energy structure may remain hard to resolve, both experimentally and theoretically, as it represents only a small energy difference resulting from the interplay between local and nonlocal interactions.

ACKNOWLEDGMENT

Support from the National Science Foundation under Contract No. CHE-0213488 is greatfully acknowledged.

[1]D. Eisenberg and W. Kauzmann, *The Structure and Properties of Water* (Oxford University Press, New York, 1969).
[2]V. F. Petrenko and R. W. Whitworth, *Physics of Ice* (Oxford University Press, New York, 1999).
[3]N. Bjerrum, Science **115**, 385 (1952).
[4]K. S. Pitzer and J. Polissar, J. Phys. Chem. **60**, 1140 (1956).
[5]O. Dengel, U. Eckener, H. Plitz, and N. Riehl, Phys. Lett. **9**, 291 (1964).
[6]G. P. Johari and S. J. Jones, J. Chem. Phys. **62**, 4213 (1975).
[7]S. M. Jackson and R. W. Whitworth, J. Chem. Phys. **103**, 7647 (1995).
[8]S. M. Jackson and R. W. Whitworth, J. Phys. Chem. B **101**, 6177 (1997).
[9]X. Su, L. Lianos, Y. R. Shen, and G. Somorjai, Phys. Rev. Lett. **80**, 1533 (1998).
[10]M. J. Iedema, M. J. Dresser, D. L. Doering, J. B. Rowland, W. P. Hess, A. A. Tsekourus, and J. P. Cowin, J. Phys. Chem. B **102**, 9203 (1998).
[11]H. Fukazawa, S. Mae, S. Ikeda, and O. Watanabe, Chem. Phys. Lett. **294**, 554 (1998).
[12]Y. Wang, J. C. Li, A. I. Kolesnikov, S. Parker, and S. J. Johnsen, Physica B **276**, 282 (2000).
[13]A. D. Fortes, I. G. Wood, D. Grigoriev, M. Alfredsson, S. Kipfstuhl, K. S. Knight, and R. I. Smith, J. Chem. Phys. **120**, 11376 (2004).
[14]R. W. Whitworth, J. Phys. Chem. B **103**, 8192 (1997).
[15]O. Wörz and R. H. Cole, J. Chem. Phys. **51**, 1546 (1969).
[16]S. Kawada and J. Niinuma, J. Phys. Soc. Jpn. **43**, 715 (1977).
[17]G. P. Johari and E. Whalley, J. Chem. Phys. **75**, 1333 (1981).
[18]Y. Tajima, T. Matsuo, and H. Suga, J. Phys. Chem. Solids **35**, 1135 (1984).
[19]O. Yamamuro, N. Kuratomi, T. Matsuo, and H. Suga, Solid State Commun. **73**, 317 (1990).
[20]M. Tyagi and S. S. N. Murthy, J. Phys. Chem. A **106**, 5072 (2002).
[21]I. Minagawa, J. Phys. Soc. Jpn. **50**, 3669 (1981).
[22]C. M. B. Line and R. W. Whitworth, J. Chem. Phys. **104**, 10008 (1996).
[23]G. T. Barkema and J. de Boer, J. Chem. Phys. **99**, 2059 (1993).
[24]A. J. Leadbetter, R. C. Ward, J. W. Clark, P. A. Tucker, T. Matsuo, and H. Suga, J. Chem. Phys. **82**, 424 (1985).
[25]S. M. Jackson, V. M. Nield, R. M. Whitworth, M. Orguro, and C. C. Wilson, J. Phys. Chem. B **101**, 6142 (1997).
[26]E. R. Davidson and K. Morokuma, J. Chem. Phys. **81**, 3741 (1984).
[27]S. Kawada, J. Phys. Soc. Jpn. **44**, 1881 (1978).
[28]I. Minagawa, J. Phys. Soc. Jpn. **59**, 1676 (1990).
[29]G. P. Johari and S. J. Jones, J. Glaciology **21**, 259 (1978).
[30]J. Lekner, Physica B **252**, 149 (1998).
[31]S. Cassassa, P. Ugliengo, and C. Pisani, J. Chem. Phys. **106**, 8030 (1997).
[32]V. Buch, P. Sandler, and J. Sadlej, J. Phys. Chem. B **102**, 8641 (1998).
[33]L. A. Báez and P. Clancy, Mol. Phys. **86**, 385 (1995).
[34]L. A. Báez and P. Clancy, J. Chem. Phys. **103**, 9744 (1995).
[35]M. J. Vlot, J. Huinink, and J. P. van der Eerden, J. Chem. Phys. **110**, 55 (1999).
[36]G. T. Gao, X. C. Zeng, and H. Tanaka, J. Chem. Phys. **112**, 8534 (2000).
[37]B. W. Arbuckle and P. Clancy, J. Chem. Phys. **116**, 5090 (2002).
[38]H. Nada and J. P. van der Eerden, J. Chem. Phys. **118**, 7401 (2003).
[39]E. Sanz, C. Vega, J. L. F. Abascal, and L. G. MacDowell, J. Chem. Phys. **121**, 1165 (2004).
[40]H. J. C. Berendsen, J. R. Grigera, and T. P. Straatsma, J. Phys. Chem. **91**, 6269 (1987).
[41]W. L. Jorgensen, J. Chandrasekhar, J. D. Madura, R. W. Impey, and M. L. Klein, J. Chem. Phys. **79**, 926 (1983).
[42]M. W. Mahoney and W. L. Jorgensen, J. Chem. Phys. **112**, 8910 (2000).
[43]J. A. Hayward and J. R. Reimers, J. Chem. Phys. **106**, 1518 (1997).
[44]A. Rahman and F. Stillinger, J. Chem. Phys. **57**, 4009 (1972).
[45]S. W. Rick and A. D. J. Haymet, J. Chem. Phys. **118**, 9291 (2003).
[46]G. T. Barkema and M. E. J. Newman, Phys. Rev. E **57**, 1155 (1998).
[47]J. F. Nagle, J. Math. Phys. **7**, 1484 (1964).
[48]J. F. Nagle, J. Chem. Phys. **61**, 883 (1974).
[49]Y. Ishibashi, J. Phys. Soc. Jpn. **63**, 3528 (1994).
[50]J. Kuo and S. J. Singer, Phys. Rev. E **67**, 016114 (2003).
[51]S. W. Rick, S. J. Stuart, and B. J. Berne, J. Chem. Phys. **101**, 6141 (1994).
[52]G. P. Johari, J. Chem. Phys. **109**, 9543 (1998).
[53]N. Metropolis, A. Rosenbluth, M. Rosenbluth, A. Teller, and E. Teller, J. Chem. Phys. **21**, 1087 (1953).
[54]S. W. Rick, J. Chem. Phys. **120**, 6085 (2004).
[55]H. C. Andersen, J. Chem. Phys. **72**, 2384 (1980).
[56]G. Ciccotti and J. P. Ryckaert, Comput. Phys. Rep. **4**, 345 (1986).
[57]G. J. Martyna, D. J. Tobias, and M. L. Klein, J. Chem. Phys. **101**, 4177 (1994).
[58]S. Nosé, Mol. Phys. **52**, 255 (1984).
[59]W. G. Hoover, Phys. Rev. A **31**, 1695 (1985).
[60]M. Parrinello and A. Rahman, Phys. Rev. Lett. **45**, 1196 (1980).
[61]M. P. Allen and D. J. Tildesley, *Computer Simulation of Liquids* (Oxford University Press, Oxford, 1987).
[62]In Ref. 45, the signs for the energy differences for the different types of hydrogen bonds are incorrect. See the text for the correct values.
[63]K. Röttger, A. Endriss, J. Ihringer, J. Doyle, and W. F. Kuhs, Acta Crystallogr., Sect. B: Struct. Sci. **50**, 644 (1994).
[64]O. A. Karim and A. D. J. Haymet, J. Chem. Phys. **89**, 6889 (1988).
[65]H. Saint-Martin, B. Hess, and H. J. C. Berendsen, J. Chem. Phys. **120**, 11133 (2004).
[66]S. W. Rick, J. Phys. Chem. **114**, 2276 (2001).
[67]M. Lisal, J. Kolafa, and I. Nezbeda, J. Chem. Phys. **117**, 8892 (2002).
[68]L. Onsager and M. Dupuis, in *Electrolytes*, edited by B. Pesce (Pergamon, Oxford, 1962), p. 27.

[69]E. R. Batista, S. S. Xantheas, and H. Jónsson, J. Chem. Phys. **109**, 4546 (1998).
[70]E. R. Batista, S. S. Xantheas, and H. Jónsson, J. Chem. Phys. **112**, 3285 (2000).
[71]L. Delle Site, A. Alavi, and R. M. Lynden-Bell, Mol. Phys. **96**, 1683 (1999).
[72]E. Whalley, J. Chem. Phys. **81**, 4087 (1984).
[73]M. Sprik, J. Chem. Phys. **95**, 6762 (1991).
[74]A. Wallqvist and R. D. Mountain, in *Reviews in Computational Chemistry*, edited by K. B. Lipkowitz and D. B. Boyd (Wiley-VCH, New York, 1999), pp. 183–247.
[75]J. Soetens, M. T. C. Martins Costa, and C. Millot, Mol. Phys. **94**, 577 (1998).
[76]S. L. Carnie and G. N. Patey, Mol. Phys. **47**, 1129 (1982).